EJN European Journal of Neuroscience

FENS Federation of European Neuroscience Societies

European Journal of Neuroscience, Vol. 48, pp. 2903–2914, 2018 doi:10.1111/ejn.13822

Effects of chronic ketamine on hippocampal cross-frequency coupling: implications for schizophrenia pathophysiology

Timothy I. Michaels, Lauren L. Long, Ian H. Stevenson, James J. Chrobak and Chi-Ming A. Chen
Psychological Sciences Department, University of Connecticut, 406 Babbidge Road, Unit 1020, Storrs, CT 06269, USA

Keywords: CA1, Long Evans, NMDA antagonism, theta-gamma coupling

Abstract

Disrupted neuronal oscillations have been identified as a potentially important biomarker for the perceptual and cognitive symptoms of schizophrenia. Emerging evidences suggest that interactions between different frequency bands, cross-frequency coupling (CFC), serve an important role in integrating sensory and cognitive information and may contribute to disease pathophysiology. In this study, we investigated the effects of 14-day consecutive administration of ketamine (30 mg/kg i.p.) vs. saline on alterations in amplitude and changes in the coupling of low-frequency (0–30 Hz) phase and high-frequency (30–115 Hz) amplitude in the CA1 hippocampus of Long Evans rats. Intracranial electrode recordings were conducted pre- and post-injection while the animals performed a foraging task on a four-arm rectangular maze. Permutation analysis of frequency band-specific change in amplitudes revealed between-group differences in theta (6–12 Hz) and slow gamma (25–50 Hz) but not fast gamma (65–100 Hz) bands at both slow and fast speeds. Chronic ketamine challenge resulted in decreased coupling (pre to post) at slow speeds but increased coupling at faster speeds, compared to either no or modest increased coupling in the saline group. These results demonstrate that chronic ketamine administration alters the interaction of low-frequency phase and high-frequency oscillations chronically and that such coupling varies as a function of locomotive speed. These findings provide evidence for the potential relevance of CFC to the pathophysiology of schizophrenia.

Introduction

The pathophysiology of schizophrenia is complex and has yet to be fully characterized despite over a century of research. Convergent evidence suggests that schizophrenia is neurodevelopmental in origin and likely involves genetic, molecular and structural abnormalities within and across diverse brain regions (Lakhan & Vieira, 2009). However, there remains a critical need to improve translational models (Wong & Josselyn, 2016) that relate neurobiological abnormalities to endophenotypes indicative of the positive (such as hallucinations and delusions), negative (such as avolition and apathy) and cognitive (impairments in memory, learning and executive functioning) symptoms (American Psychiatric Association, 2013) that characterize the disease. One of the most promising avenues for doing so may be through developing a more precise understanding of how neural oscillations functionally contribute to the cognitive and information processing deficits central to schizophrenia (Uhlhaas & Singer, 2010).

Neural oscillations have been posited to play a role in both sensory integration (Engel *et al.*, 2001) and cognition (Hirai *et al.*, 1999). However, the precise mechanisms by which different rhythms coordinate neural activity within and across brain networks remain unclear (Ward, 2003). Oscillations at lower frequencies, such as theta (6–12 Hz) rhythms, coordinate neural activity on a relatively slow time scale and therefore are a prime candidate for synchronizing neurons across widespread networks (Burgess & O'Keefe, 2005). Faster waves, such as gamma (25–140 Hz) oscillations, organize spatially distributed local subpopulations of neurons to form temporally defined ensembles (Chrobak & Buzsáki, 1998) thereby facilitating the representation, storage and retrieval of information (Fell *et al.*, 2001). Interestingly, gamma oscillations co-occur (and are strongest) with theta rhythms in the hippocampus (Bragin *et al.*, 1995; Belluscio *et al.*, 2012), a brain region critical for learning and memory (Andersen *et al.*, 2009) that is central to schizophrenia pathophysiology (Harrison, 2004). There is strong evidence of reduced gamma-band amplitude in the hippocampus of patients with schizophrenia (Schmiedt *et al.*, 2005; Haenschel *et al.*, 2009), and oscillatory alterations have been reported in both first-episode (Spencer *et al.*, 2008; Williams *et al.*, 2009) and early-onset patients (Wilson *et al.*, 2008) as even in those at high risk for psychosis (Leicht *et al.*, 2016). Animal models of the disease consistently report reduced hippocampal theta amplitude (Hinman *et al.*, 2012),

Correspondence: Timothy I. Michaels, as above. E-mail: timothy.michaels@uconn.edu

Received 22 June 2017, revised 4 January 2018, accepted 11 January 2018

Edited by Gregor Thut. Reviewed by Jordan Hamm, Columbia University, USA; and Miles Whittington, University of York, UK

All peer review communications can be found with the online version of the article.

specifically in area CA1 (Leung & Shen, 2004; Kittelberger *et al.*, 2012; Caixeta *et al.*, 2013).

Several studies (Sirota *et al.*, 2008; Colgin *et al.*, 2009) provide evidence suggesting distinct functional roles for the entrainment of gamma oscillations by hippocampal theta rhythms. In CA1 hippocampus, the amplitude of slow and fast gamma oscillations is modulated by different phases of theta oscillations (Tort *et al.*, 2010; Scheffer-Teixeira *et al.*, 2012), which suggests that theta rhythms integrate gamma-mediated cell assemblies across space and time. Colgin *et al.* (2009) demonstrated that slow and fast variants of CA1 gamma temporally integrate sensory and perceptual information in a task-relevant manner. While CA1 fast gamma (65–100 Hz) oscillations are coherent with gamma oscillations in medial entorhinal cortex, which transmits sensory and perceptual information about the current environment to the hippocampus (Hafting *et al.*, 2005; Fyhn *et al.*, 2007), slow gamma (25–50 Hz) CA1 rhythms are coherent with gamma oscillations in CA3 (Colgin *et al.*, 2009), an area critical for memory retrieval (Sutherland *et al.*, 1983; Steffenach *et al.*, 2002). Theta-gamma coupling thus appears to play an important role in the formation of a neural code that tags perceptual information critical for short-term memory (Vertes, 2005; Lisman & Buzsáki, 2008).

Interestingly, patients with schizophrenia demonstrate consistent impairments in spatial working memory (Fleming *et al.*, 1997; Silver & Goodman, 2008; Brébion *et al.*, 2015), yet it remains unclear whether disrupted hippocampal theta-gamma coupling relates to the underlying pathology of such deficits. In animal models of schizophrenia, acute administration of N-methyl-aspartate receptor (NMDAR) antagonist drugs, such as ketamine, reliably produces behavioral and neurobiological alterations consistent with clinical pathology (Krystal *et al.*, 1994; Imre *et al.*, 2006; Roopun *et al.*, 2008; Hakami *et al.*, 2009; Kittelberger *et al.*, 2012) including reduction in the number of hippocampal parvalbumin-positive interneurons (Cunningham *et al.*, 2006). While some aspects of schizophrenia are well modeled by acute ketamine doses in humans (Krystal *et al.*, 1994), others are better modeled chronic drug exposure (Behrens *et al.*, 2007; Javitt *et al.*, 2012). In chronic animal models, knockout of the NMDAR1 gene in CA1 hippocampus results in impaired spatial memory (Tsien *et al.*, 1996) and ablation of parvalbumin-positive interneurons disrupts both theta and gamma oscillations (Korotkova *et al.*, 2010), suggesting a critical role for NMDAR functioning in facilitating the theta-gamma coupling that contributes to hippocampal-dependent information storage and retrieval. Several recent studies (Lazarewicz *et al.*, 2010; Hinman *et al.*, 2012; Caixeta *et al.*, 2013) have demonstrated that acute ketamine administration increases gamma-band and reduces theta-band amplitude in the rat hippocampus.

While the acute ketamine model has been validated for examining the relation of NMDAR hypofunction on specific symptoms of schizophrenia (Adell *et al.*, 2012), investigating chronic effects may contribute to improved understanding of the pathogenesis of NMDAR hypofunction and its role in abnormal oscillatory. Here, we examined the acute (within-day) and acute chronic (repeated daily administration) effects of ketamine on CA1 hippocampal theta-gamma coupling in Long Evans rats over a 14-day period. Specifically, we investigate longitudinal changes in the strength and pattern of coupling between low-frequency phase (1–30 Hz) and high-frequency amplitude (30–115 Hz) as a function of animal locomotive speed [slow (0–15 cm/s) and fast (37.5–87.5 cm/s)] and by CA1 layer. We also explored whether these chronic alterations were accompanied by frequency band-specific changes in theta (6–12 Hz), slow gamma (25–50 Hz) and fast gamma (65–100 Hz) amplitude.

Methods

Animals

The Institutional Animal Care and Use Committee (IACUC) of the University of Connecticut approved all animal care and surgical procedures. Six adult male 7–8 month-old Long Evans rats (Charles River Laboratories, Wilmington, MA) were used in the experiment. Six adult male Long Evans rats (7–8 months old) weighing 300–400 g at the time of surgery were used in the experiment randomized to either the ketamine condition ($N = 4$) or saline condition ($N = 2$). For behavioral training, rats were housed in individual polyethylene cages in a colony room and maintained on a 12-h light–dark cycle with free access to water. During training and testing, rats were food restricted to approximately 85% of their free-feeding weight by limiting their access to chow to ~30 g/day in addition to their consumption of food rewards on the maze apparatus. Rats were allowed to gain 5–10 g weight/week until they reached 500 g as which point they were food restricted to ~20 g/day in addition to their consumption of food rewards on the maze.

For surgical procedures, rats were anesthetized with isoflurane (3–5% induction; 1–3% maintenance) with both pre- and post-surgical treatment with meloxicam (1 mg/kg). Following a scalp incision, burr holes were drilled in the skull over the hippocampus. All electrode arrays were comprised of four linearly spaced 50-μm tungsten wires (12 electrodes per animal; California Fine Wire Company, Grover Beach, CA). Electrode wire was arranged and separated by fused silica tubing (Polymicro Tubing, Phoenix, AZ), attached to female pins (Omnetics, Minneapolis, MN) and secured in a rectangular four by four pin array. Two stainless steel watch screws driven into the skull above the cerebellum served as indifferent and ground electrodes [see (Hinman *et al.*, 2012; Penley *et al.*, 2013; Long *et al.*, 2016) for additional details]. Supplementary anchor screws were positioned anteriorly, and the entire head-stage ensemble was fortified with dental acrylic. Arrays were positioned to target the septal axis of the CA1 region of the hippocampus using the following coordinates: AP: −3.0 to −4.0 mm; ML: 2.0–3.0 mm; DV: 2.0–3.0 mm relative to bregma. Electrode placements spanned from the stratum oriens layer to the stratum lacunosum moleculare (Slm) layer of CA1 hippocampus.

Upon completion of the study, animals were transcardially perfused with ice-cold saline followed by 4% paraformaldehyde in 0.1 M phosphate buffer. The brains were sliced using a vibratome and then mounted and stained with thionin. Each electrode position was placed on a flatmap representation of the hippocampus (Swanson & Cowan, 1977) to verify the placement (within each layer and across the septotemporal axis) and distance between electrodes. For each electrode track, a photomicrograph was taken and digitized with different colored dots representing electrode positions for each animal (Fig. 1A).

Behavioral data collection and drug administration

Following recovery from surgery, drugs were administered on a daily basis while electrophysiological/behavioral recordings were conducted pre- and post-injection on days 1, 3, 5, 7, 9, 10, 12 and 14. For daily injections, Ketamine hydrochloride (Ketaset, 100 mg/mL; Fort Dodge Laboratories, Fort Dodge, IA) was prepared in physiological saline (0.9% sterile solution), and all injections of ketamine (30 mg/kg) or saline were administered intraperitoneally in volumes of 1 mL/kg. This dose of ketamine is well below the anesthetic dose (200 mg/kg IP) in adult rats (Green *et al.*, 1981).

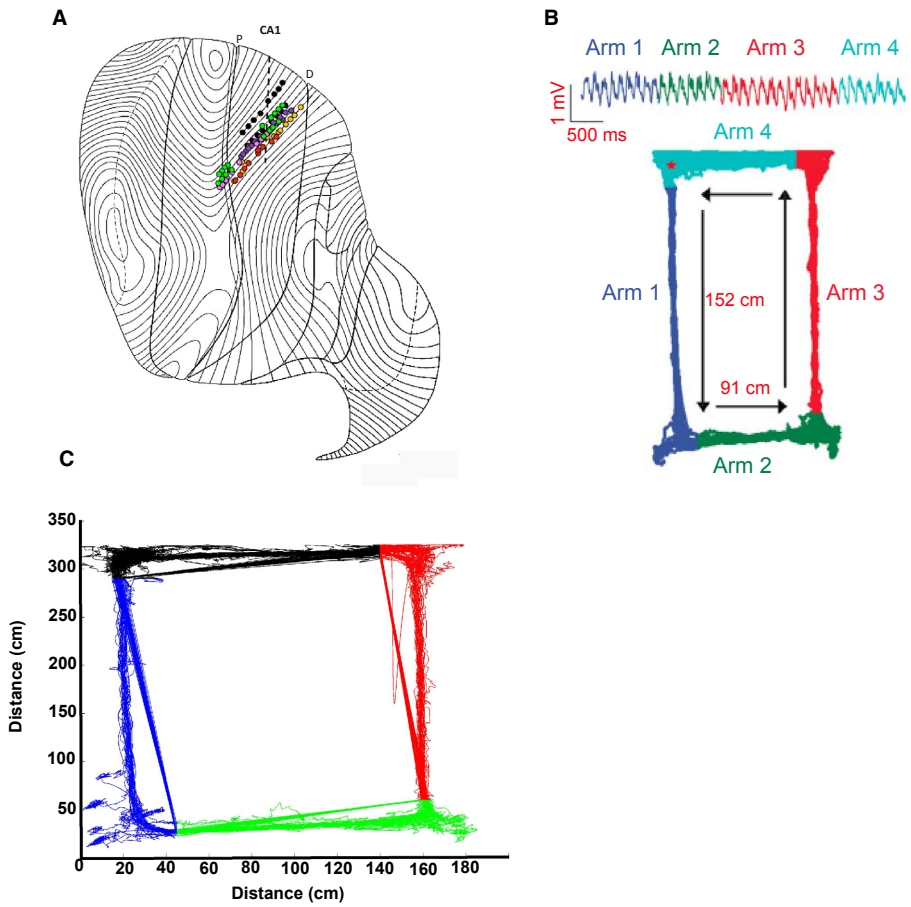

FIG. 1. Flatmap representation of electrode placement in all animals in CA1 hippocampus from proximal (P) to distal (D) from the stratum lacunosum moleculare (Slm) to stratum orients (SO) layers. Blue, pink, red and yellow dots represent ketamine rats, and green and black dots represent saline animals (A). Animals were trained for 3 months to run counterclockwise around a 152 × 91 cm^2 rectangular track for a chocolate chip food reward located in the northwest corner of the maze (B). Sample plot of speed data from a single electrode from one animal at a single time point (C). A camera located above the maze tracked animal movement through light-emitting diodes attached to the animal's head stage. Speed was computed using the finite difference between successive tracking (position) samples.

Over a 3-month period, animals were trained to run counterclockwise on a four-arm rectangular track (152 × 91 cm^2). Animals were rewarded with a chocolate chip located in the northwest corner of the maze (Fig. 1B). Two 10-min recordings were conducted per day on eight separate days spanning a period of 2 weeks. Animals continued to receive injection on intermediary days in which data were not recorded. Pre-injection recordings (pre) were conducted prior to daily drug administration, and post-injection (post) recordings were conducted approximately 10 min after the injection. During each recording session, we recorded wideband electrical activity (1–1894 Hz, sampling rate of 3787 Hz) using a Neuralynx (Bozeman, MT) data acquisition system (Chang *et al.*, 2013). While the rats were completing the behavioral task, a camera located above the maze tracked each animal movement through monitoring light-emitting diodes attached to the animal's head stage.

Data analysis: signal processing

Electrodes with significant interference or poor recording quality (n = 37) were excluded from the analysis. Recording quality was determined through visual inspection of the raw LFP signal. Those electrodes with flat signals or that frequently switched offline for the majority of the recording were presumed to have been damaged during the fabrication or implantation and therefore were excluded from analysis. This resulted in a final total of 42 electrodes analyzed in the ketamine group and 17 electrodes analyzed in the saline group (total = 59 electrodes or 82% of implanted electrodes). For the purpose of analyzing changes in oscillatory amplitude as an effect of chronic ketamine administration, each electrode within an animal was treated as separate and independent rather than averaging values across all electrodes within an animal.

All signal processing and related procedures (including amplitude and cross-frequency coupling analysis) were performed using custom scripts in MATLAB (MathWorks, 2014). Statistical analyses were performed in *R* (R Core Development Team, 2013) and SPSS (IBM SPSS Inc., 2012). Both the local field potential (LFP) recordings and speed data were resampled at a rate of 631.3133 Hz. Speed data were cubic spline interpolated to match the time points of the electrophysiology data. Speed was computed using the finite difference between successive tracking (position) samples, normalized by the sampling period and following a low-pass filter to minimize head movements and other artifact. The raw LFP signal was bandpass-filtered between 6 and 12 Hz (Theta), 25–50 Hz (Slow Gamma) and 65–100 Hz (Fast Gamma) using a Hilbert transformation to extract the envelope. We then calculated the average amplitude for each of the three bands for each electrode at all time points (days 1, 3, 5, 7,

9, 10, 12 and 14; pre and post) for a total of 16 time points. To the remove the influence of any extreme data points, we conducted an outlier analysis for each electrode (within each time point) that removed any speed values ±2.5 standard deviations from the animal's average speed during the session. The outlier analysis removed approximately 1% of the data. The time points associated with the removed speed outliers were matched to and removed from the LFP data at each of the three frequency bands.

Given the putative role of CA1 hippocampal oscillations in sensorimotor integration and locomotive speed (Imre *et al.*, 2006; Penley *et al.*, 2013; Long *et al.*, 2015), drug-induced changes in animal speed served as the study's primary behavioral measure. Hippocampal theta power has been shown to be larger when animals are engaged in locomotion (Burgess & O'Keefe, 2005; Jones & Wilson, 2005; Long *et al.*, 2015). Yet ketamine administration is known to alter locomotor speed in rats (Hetzler & Swain Wautlet, 1985; Ma & Leung, 2007), in an independent manner that can be reliably distinguished from the drug's electrophysiological effects (Hakami *et al.*, 2009). Notably, repeated administration does not appear to cause a day-dependent increase in locomotor activity (McDougall *et al.*, 2017). Indeed, speed distributions across a subset of days demonstrate that animals in the ketamine group (Fig. 2A) spent more time at fast speeds during post-injection sessions relative to pre-injection sessions. This finding was not observed in the saline group (Fig. 2B) despite the fact that median speed increased from pre to post in both groups (Fig. 2C). To account for these speed differences within the context of ketamine-induced oscillatory changes, all amplitude and cross-frequency coupling analyses were conducted separately at both slow (0–15 cm/s) and fast (37.5–87.5 cm/s) speeds. These two ranges were chosen based on visually inspecting the log-transformed speed distributions of both groups (at all time points), which indicated a bimodal distribution with modes centered at 7.5 cm/s (slow) and 62.5 cm/s (fast).

Percent change in average amplitude ((post-pre)/pre) over time was analyzed by fitting a trend line ($y = a + b*\exp(-t/\tau)$) to the longitudinal data with multiple ($n = 1024$) bootstrap permutations, where a denotes a constant offset, b is the amplitude of the exponential trend, and τ is the time constant. Trend lines were fit separately for each group (saline or ketamine), each frequency band (theta, slow gamma and fast gamma) and at differing (slow or fast) speeds (i.e., $2 \times 3 \times 2$). Alpha levels were adjusted for multiple comparisons by applying a Bonferroni correction (adjusted alpha level, $P < 0.002$). Statistical results are reported for differences in baseline (offset) and changes across time (exponential) separately for each group and each frequency band (Fig. 4). If there were significant differences (for either baseline or exponential) in both groups, we performed a bootstrap test (Bonferroni-corrected alpha level of 0.004) to determine whether the distributions differed significantly between groups.

Data analysis: cross-frequency coupling

Given important differences in LFP signaling (Scheffer-Teixeira *et al.*, 2012) and the strength and pattern of CFC (Belluscio *et al.*, 2012) across CA1 layers, the CFC analysis was conducted separately for groupings of electrodes based on implantation location (see

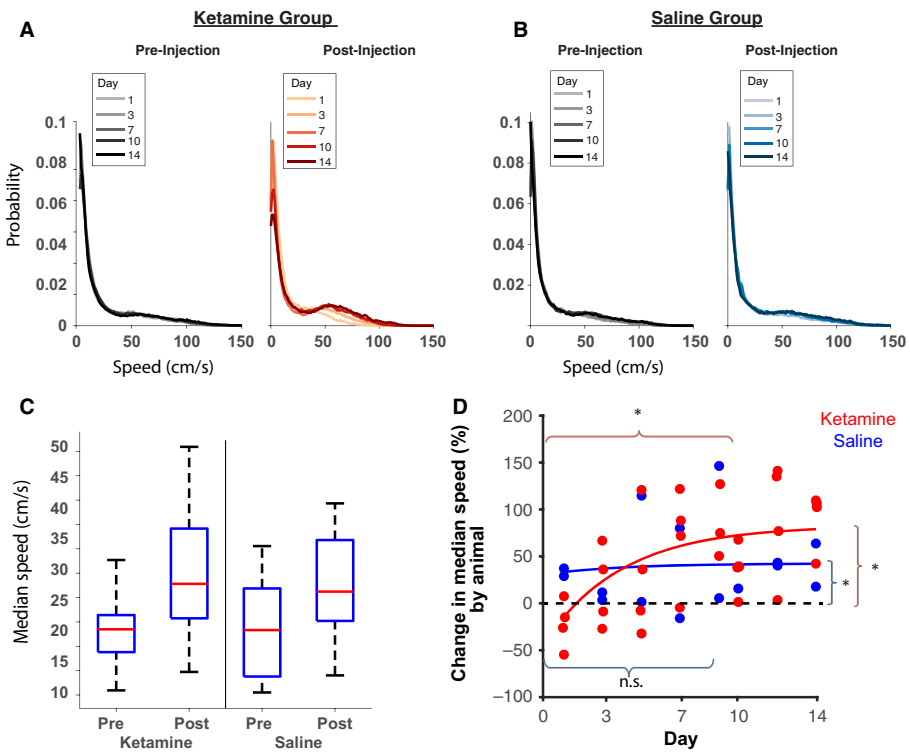

FIG. 2. Probability distribution of animal locomotive speed for on days 1, 3, 7, 10 and 14. In the ketamine group (A), the animals spend more significantly more time at fast speeds (> 15 cm/s) post-injection compared to pre-injection across days. In the saline group (B), the animals do not spend significantly more time at fast speeds ($P = 0.46$). Overall, the median speed (C) post-injection is higher compared to pre-injection speed in both groups. Change in median speed was analyzed across all days (D) and demonstrated a significant exponential trend over time for the ketamine but not the saline group. Both groups differed significantly from zero at baseline. n.s., not significant. *$P < 0.002$ (Bonferroni-corrected alpha level). Brackets indicate significance tests for exponential (x-axis) or baseline (y-axis) changes (red = ketamine group; blue = saline group).

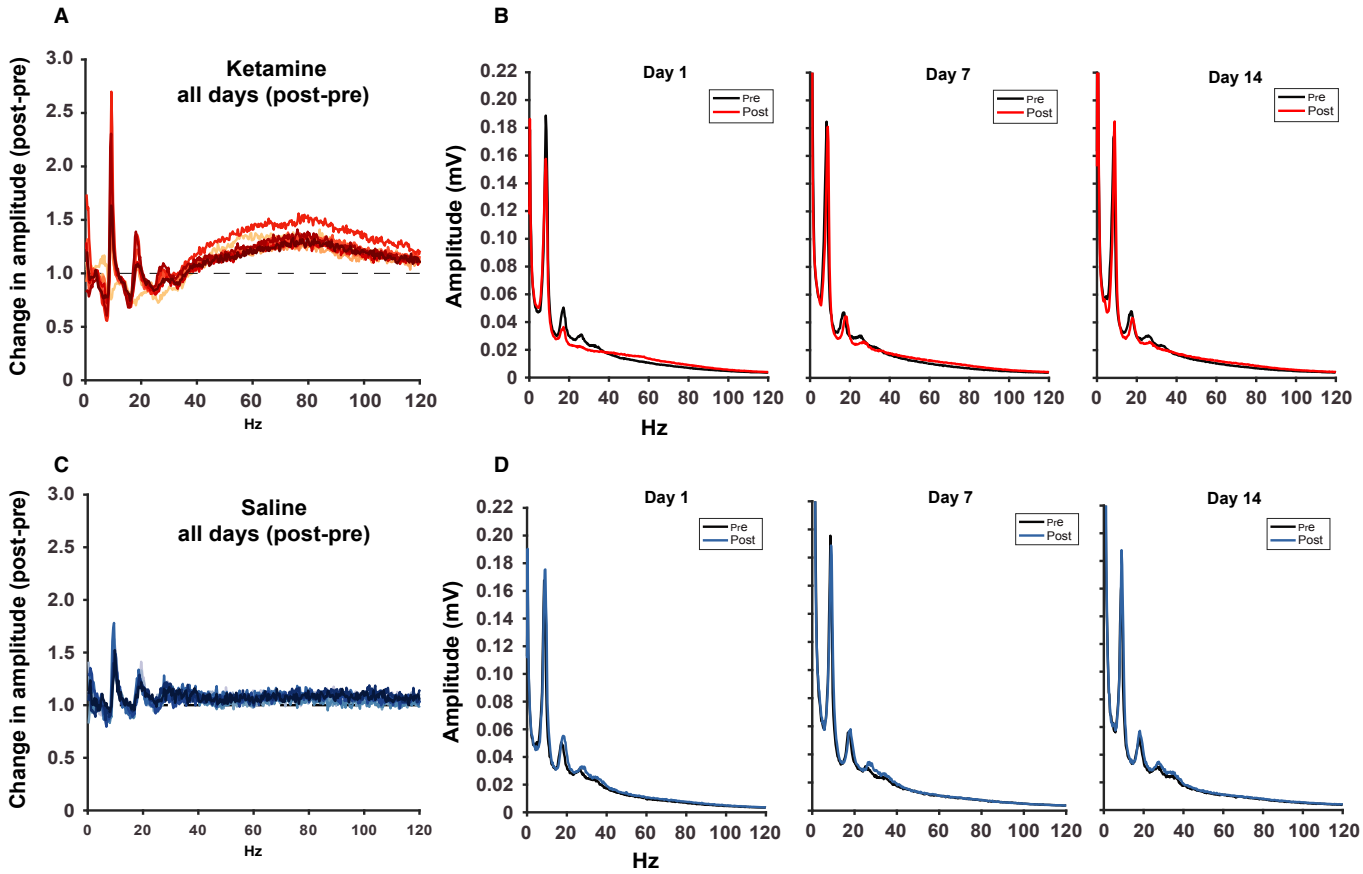

FIG. 3. Percent change local field potential (LFP) spectral density plot by injection group. In the ketamine group (A), there is an increase in both the theta (6–12 Hz) and gamma (25–100 Hz) band frequency. This difference between pre- and post-injection is also apparent when comparing the LFP signal separately on days 1, 7 and 14 (B). While there are also apparent changes in the saline group (C), these occur primarily at lower frequencies. Closer examination of the LFP signal for the saline group on days 1, 7 and 14 indicates similar amplitudes (D) between pre- and post-injection electrophysiology data across the spectral band.

Fig. 1). Electrodes within a given layer were included in the analysis if there were at least one electrode in at least two animals within each group (saline or ketamine). This resulted in 17 electrodes analyzed in the stratum lacunosum moleculare (Slm) layer (ketamine = 11, saline = 6), 23 electrodes in the stratum radiatum (Sr) layer (ketamine = 15; saline = 8) and five electrodes analyzed in the stratum pyramidale (Pyr) layer (ketamine = 2, saline = 3). There were an insufficient number of electrodes implanted in either the alveus (Alv) or stratum oriens (So) layer to meet the above requirements, and therefore, these electrodes (n = 7) were excluded from the CFC analysis.

The raw LFP signal was bandpass-filtered between 1 and 115 Hz in using a Hilbert transformation to extract the envelope. We used the mean vector length modulation index (MVL-MI) methodology described previously (Canolty *et al.*, 2006) to assess phase-amplitude CFC. The amplitude envelope time series of the high-frequency band (30–115 Hz) was combined with the phase time series of the low-frequency (1–30 Hz) band into one composite, complex-value signal. The raw modulation index was then computed as the mean vector length (modulus) of the high-frequency amplitude and low-frequency phase at each sampled time point. Because the vector length is dependent on signal amplitude, raw modulation indices were normalized through a z-score transformation using the mean and standard deviation within each day (across pre and post) and within each animal. For a subset of time points (day 1, 3, 7, 10 and 14), we created a comodulation map that expresses the change (post–pre) in coupling strength (MVL-MI index) for each frequency band pair in a pseudocolor plot. The change in coupling is presented separately by layer and injection at slow and fast speeds.

Results

We first examined changes in locomotive speed over time and differences (pre to post) between groups. Speed distributions across a subset of days demonstrate that animals in the ketamine group (Fig. 2A) spent more time at fast speeds during post-injection sessions relative to pre-injection sessions. This finding was not observed in the saline group (Fig. 2B) despite the fact that median speed increased from pre to post in both groups (Fig. 2C). Permutation analysis of change in median speeds across time shows significant baseline differences in both groups ($P < 0.001$) but only exponential differences in ketamine ($P < 0.001$) and not saline ($P = 0.128$) animals (Fig. 2D).

Prior to statistically analyzing band-specific changes in oscillatory amplitude, we examined changes (post–pre) in the overall LFP signal across all days and between groups. In the ketamine group, there was a consistent increase in amplitude across days that appeared to be most prominent in the theta (6–12 Hz) and fast gamma (65–100 Hz) band frequencies (Fig. 3A). A closer examination of both the pre- and post-injection signal at days 1, 7 and 14 suggests that these may larger at day 1 (Fig. 3B). While there were also changes in amplitude across the

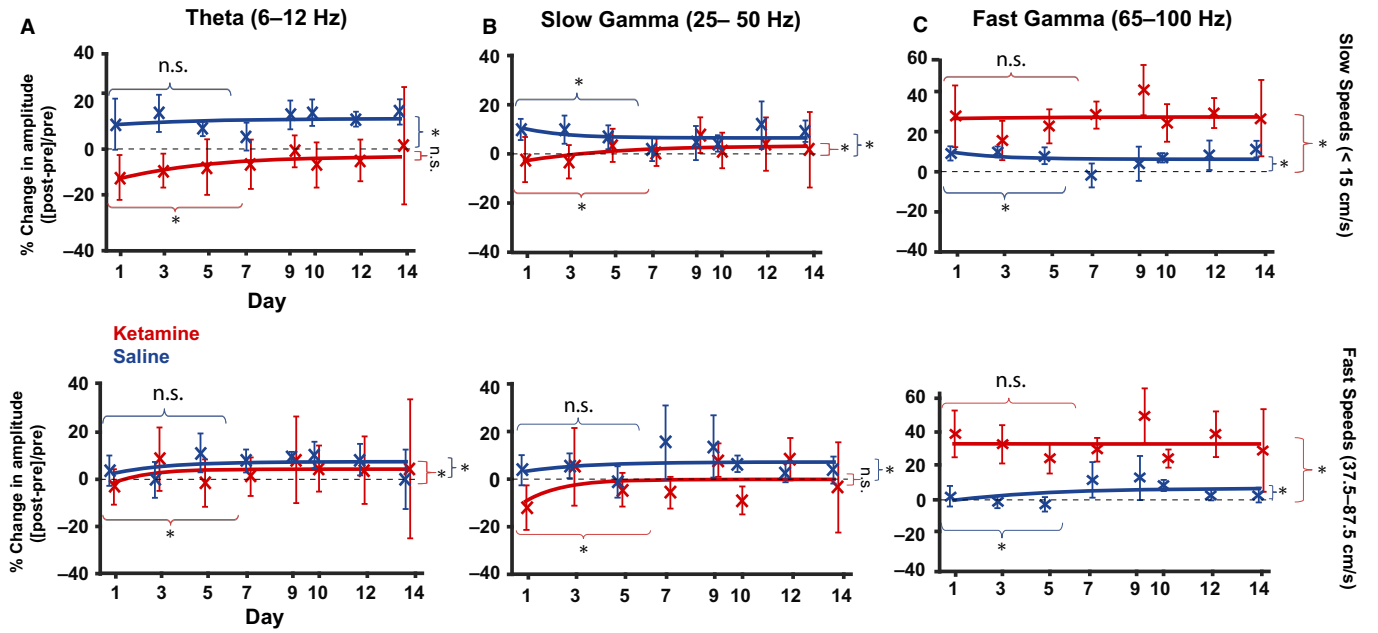

FIG. 4. Mean and standard deviation of average amplitude by day and speed group for theta (A), slow gamma (B) and fast gamma (C) amplitude. Top row reflects amplitude data at slow speeds (< 30 cm/s), and the bottom row represents results at fast speeds (37.5–87.0 cm/s). Statistical results are shown for baseline (offset) from zero by group and for exponential trend by group. n.s., not significant; *$P < 0.002$ (Bonferroni-corrected alpha level). Brackets indicate significance tests for exponential (*x*-axis) or baseline (*y*-axis) changes (red = ketamine group; blue = saline group).

LFP signal in the saline group, they appeared to be of a much smaller magnitude (Fig. 3C) and were primarily limited to lower frequencies (Fig. 3D). To statistically characterize these alterations in the LFP signal (pre- to post-injection), we utilized a permutation test to analyze baseline and exponential changes in theta (6–12 Hz), slow gamma (25–50 Hz) and fast (65–100 Hz) gamma-bands as a function of both slow (< 15 cm/s) and fast (37.5–87.5 cm/s) locomotive speeds.

Changes in theta amplitude

To characterize changes in theta frequency band, we examined between-group differences in the percent change in amplitude [(post-pre)/pre] across all days at both slow and fast speeds, predicting both acute and chronic decreases in theta power. At slow speeds, the baseline for theta amplitude decreased 3.1 ± 1.3% in the ketamine group ($P = 0.009$, *n.s.*) and increased 13.0 ± 0.8% in the saline group ($P = 0.001$). The exponential for theta amplitude declined by 9.1 ± 3.5% ($P = 0.001$) in the ketamine group and by 2.2 ± 2.9% in the saline group ($P = 0.269$, *n.s.*). At fast speeds, the baseline for theta amplitude increased 4.6 ± 1.4% in the ketamine group ($P = 0.001$) and by 7.5 ± 0.9% in the saline group ($P = 0.001$). Baseline theta amplitude at fast speeds did not differ between groups ($P = 0.047$). The exponential for theta amplitude declined by 5.9 ± 2.5% in the ketamine group ($P = 0.001$) and by 5.2 ± 1.9% in the saline group ($P = 0.004$, *n.s.;* Fig. 4A). Overall, there was an apparent trend over time for the ketamine group, with decreases in theta amplitude at slow speeds and increases at fast speeds. This is somewhat inconsistent with other studies (Kittelberger *et al.*, 2012) that report a chronic decrease in theta amplitude over a similar time period.

Changes in slow gamma amplitude

Consistent with previous findings, we hypothesized that chronic ketamine would result in increased slow gamma amplitude at both slow and fast speeds. The baseline for slow gamma amplitude increased 3.4 ± 1.1% in the ketamine group ($P = 0.001$) and 6.5 ± 0.7% in the saline group ($P = 0.001$) at slow speeds, although there was no significant difference in baseline slow gamma amplitude between groups ($P = 0.009$). At slow speeds, the exponential decreased 5.8 ± 2.9% in the ketamine group ($P = 0.001$) but increased by 4.0 ± 1.3% ($P = 0.001$) in the saline group. Interestingly, this difference was significantly larger in the ketamine group ($P = 0.001$). For fast speeds, the baseline of slow gamma amplitude decreased by 0.1 ± 0.9% in the ketamine group ($P = 0.461$, *n.s.*) but increased 7.2 ± 1.0% in the saline group ($P = 0.001$). At fast speeds, the exponential for slow gamma decreased by 8.7 ± 3.5% in the ketamine group ($P = 0.001$) and decreased 4.0 ± 1.9% in the saline group ($P = 0.016$, *n.s.*; Fig. 4B). Overall, while there were significant between-group differences in slow gamma amplitude at both speeds, the magnitude of these differences was relatively small when compared to the magnitude in other frequency bands. In contrast to previous studies that find an acute increase, followed by a chronic decrease in gamma amplitude, the largest decreases occurred on days 1 and 3, with either no or small increases on subsequent days.

Changes in fast gamma amplitude

Similar to predictions for slow gamma amplitude, we examined differences in the percent change in fast gamma amplitude over time and between groups, anticipating that ketamine administration would chronically increase fast gamma amplitude. At slow speeds, the baseline for fast gamma amplitude increased 27.8 ± 1.3% in the ketamine group ($P = 0.001$) and 6.3 ± 0.7% in the saline group ($P = 0.001$), although these changes did not differ significantly by group. The exponential for fast gamma amplitude decreased 2.3 ± 3.4% ($P = 0.037$, *n.s.*) in the ketamine group but increased 3.6 ± 1.2% in the saline group ($P = 0.001$) at slow speeds. At fast speeds, baseline fast gamma amplitude increased 31.8 ± 1.0% in

the ketamine group ($P = 0.001$) but only 6.7 ± 1.0% in the saline group ($P = 0.001$). Similar to slow speeds, although the exponential change in the ketamine group was not significantly larger than the change in the saline group, the exponential for fast gamma amplitude increased 2.4 ± 3.0% in the ketamine group ($P = 0.037$, *n.s*) but decreased 7.1 ± 1.7% in the saline group ($P = 0.001$). While the magnitude of increases in fast gamma amplitude was larger in the ketamine group, these increases did not vary significantly across repeated administration. Furthermore, although change in baseline amplitude was significantly different in the ketamine animals, it did not differ from the saline animals in which there was also a significant change in baseline amplitude. This finding contrasts with previous studies that report fast gamma amplitude increases although notably not all studies included control animals.

Cross-frequency coupling analysis

Before reviewing chronic (longitudinal) changes (post–pre) in CFC, we examined the overall pattern in coupling by group, layer and speed, averaged across all days (Fig. 5). At slow speeds, two distinct coupling patterns emerged—the first was centered below 60 Hz amplitude frequency (between 5–15 Hz phase frequency), while the other was centered above 60 Hz amplitude frequency within the same phase frequency range. In the saline group, there was an increase in coupling strength from pre to post, while there was a decrease in coupling strength in the ketamine group. This effect was generally consistent across all layers (Fig. 5A).

At fast speeds, the two patterns described above occurred in the saline group but consisted of a single continuous coupling pattern (across 40–115 Hz amplitude) in the ketamine group. The strength of the coupling differed from that at slow speeds; while coupling increased in both groups from pre to post, this increase was larger in the ketamine group compared to the saline group (Fig. 5B). Unlike at slow speeds, changes in coupling strength differed by layer within the ketamine group, with the strongest increase occurring in Pyr, followed by the Sr, and the smallest increase occurring in Slm (Fig. 5B).

Changes in CFC across CA1 layers at slow speeds

Next, we examined changes (post–pre) in the strength and pattern of phase-amplitude coupling at slow speeds (< 15 cm/s) across days (1, 3, 7, 10 and 14) and between groups (Fig. 6). Within the Pyr layer, there was an increase in coupling strength in the saline group across all days; however, the pattern was restricted to lower amplitude frequencies on days 1, 7 and 10 but included higher amplitude frequencies (above 60 Hz) on days 3 and 14 (Fig. 6A). In contrast, there was an overall decrease in coupling in the Pyr layer in the ketamine group (within the same amplitude frequency range as the saline pattern) on days 3, 7, 10 and 14. However, on day 1 (baseline), a different pattern emerged such that there was a large increase in coupling in the ketamine group between 60–100 Hz amplitude and 5–10 Hz phase frequency, with no such increase in the saline group.

Coupling patterns for electrodes implanted in the Sr layer were broadly similar to those described in Pyr; however, the increased coupling above 60 Hz amplitude also occurred on day 3 and to a lesser extent on day 7 in the ketamine group (Fig. 6B). In the ketamine group on day 1, there was an increase in coupling (rather than the decrease that occurred in Pyr) above 60 Hz. Overall, the magnitude of changes in coupling strength in both groups appeared reduced in the Sr layer compared to changes in Pyr. These findings remained consistent for electrodes placed in Slm; overall, there was an increase in coupling strength in the saline group, accompanied by decreases in coupling strength in the ketamine group (Fig. 6C). The location of the coupling patterns in Slm was consistent with those in Pyr and appeared of similar magnitude. As with the coupling in Pyr and Sr layers, day 1 remains a notable exception to this trend; where there was an increase in coupling strength in both groups, the location of the patterns differed, with the ketamine pattern occurring at higher amplitude frequencies than the saline. It is possible that this could be due to differences in behavior, including those that are not accounted for by locomotion.

Changes in CFC across CA1 layers at fast speeds

The strength and pattern of phase-amplitude coupling differed at fast speeds also illustrated differences in baseline (day 1) coupling relative to subsequent days. On day 1, there was a decrease in coupling strength in the ketamine group across all layers, predominantly between 30 and 90 Hz amplitude frequencies (Fig. 7). This was accompanied by an increase in coupling in the saline group at similar frequencies. In Pyr and Slm, but not Sr, there was also an increase in coupling strength that occurred above 90 Hz. This baseline pattern differed considerably from coupling on the following days—while in the saline group, there was almost no change from coupling strength from pre to post (except for an increase on day 7), there was a consistent increase in coupling in the ketamine group across all days. The magnitude of the ketamine-induced increase varied by layer, with the largest increase occurring in Pyr (Fig. 7A), followed by Sr (Fig. 7B) and Slm (Fig. 7C) layer. While in the saline group, there were two coupling patterns, one centered above and the other below 60 Hz amplitude, there was a single ellipsoid-shaped pattern across 40–100 Hz amplitude in the ketamine group. This between-group difference in coupling pattern was evident across all layers.

Discussion

Convergent evidence suggests that the pathophysiology of schizophrenia likely results from impairments in the temporal integration of information; however, less is known regarding the specific neural mechanisms by which such processing is disrupted. In the present study, we investigated the longitudinal effects of repeated administration of the NMDAR antagonist ketamine on phase-amplitude coupling in CA1 hippocampus. These electrophysiological alterations were examined relative to behavioral differences in locomotive speed. In the present study, we find that chronic ketamine decreases phase-amplitude coupling at slow speeds while increasing coupling at fast speeds, compared to either no or smaller increase in coupling strength in the saline group at either speed. Between-group differences in coupling strength also varied at baseline (acute, day 1) relative to subsequent (chronic over acute) injections; at slow speeds, there was an increase in coupling strength in the ketamine group at day 1 but decreased strength on subsequent days. The opposite pattern occurred at fast speeds, with decreased coupling on day 1, but increased coupling on the following days in the ketamine group. These results demonstrate that repeated ketamine administration differentially alters the interaction of low-frequency phase and high-frequency oscillations longitudinally and varies as a function of locomotive speed. Variability in coupling strength across differed by CA1 layer; while at slow speeds, the largest decreases were evident in Slm for the ketamine group, the largest increases occurred in Pyr at fast speeds.

Although there were also longitudinal group differences in band-specific amplitudes, these changes were not as sensitive to behavioral differences. While exponential changes (longitudinally) in theta and

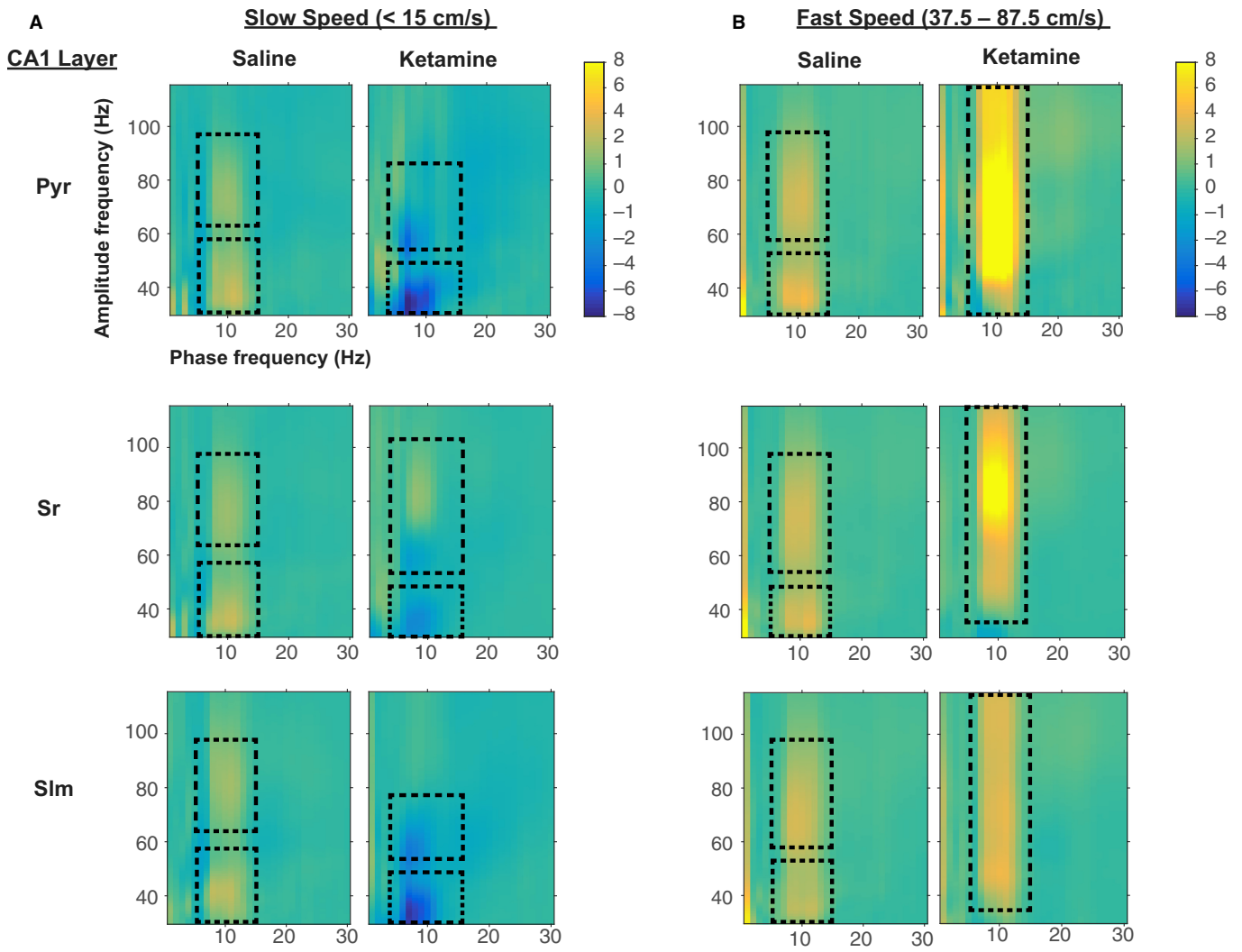

FIG. 5. Cross-frequency coupling between low-frequency (0–30 Hz) phase and high-frequency (35–110 Hz) amplitude for slow and fast speeds for ketamine and saline animals for all electrodes implanted across three CA1 layers (Pyr, stratum pyramidale; Sr, stratum radiatum; Slm, stratum lacunosum moleculare). Each plot reflects the modulation index (MI) value after subtracting post-injection from pre-injection CFC plots. At slow speeds (A), coupling strength is larger post-injection in the saline group compared to the ketamine group although the pattern in the ketamine group appears to be centered at a lower phase frequency. At fast speeds (B), the difference in CFC coupling pattern is larger in the ketamine group for the Pyr and Sr layers. The coupling is also centered at a higher phase frequency than the saline pattern.

slow gamma-band amplitudes were larger in the ketamine group compared to saline at both slow and fast speeds, this between-group difference was not evident in the fast gamma-band. There were also no instances in which baseline changes in amplitude were significantly larger in the ketamine group, compared to saline, for any frequency band.

Following NMDAR blockage by ketamine, we observe CA1 hippocampal phase-amplitude coupling differently across time and varying according to CA1 layer and animal locomotive speed. Previous studies have demonstrated that ketamine acutely increases theta phase-gamma amplitude coupling differentially across CA1 layers (Caixeta *et al.*, 2013); however, changes in phase-amplitude coupling were not studied as a function of locomotion. Furthermore, the decreased coupling observed here has only been reported at higher doses. Differences between acute (baseline) and chronic effects (on top of acute) have important implications for modeling schizophrenia pathophysiology. Furthermore, chronic ketamine appears to alter amplitude coupling in both the slow and fast gamma frequencies, which suggests that upon ketamine challenge, gamma-relevant cell ensembles in CA1 are differentially altered by NMDA antagonism, in contrast with hippocampal fast-spiking interneurons (Jones & Bühl, 1993). These region-specific coupling patterns may be associated with distinct functional differences; while fast gamma coupling has been hypothesized to coordinate information processing in the entorhinal–hippocampal–mPFC network (Miller & Cohen, 2001), slow gamma coupling is thought to be involved in memory retrieval and working memory (Sutherland *et al.*, 1983; Steffenach *et al.*, 2002). Collectively, these findings provide evidence that region-specific changes in oscillations across multiple nested frequencies may provide a more precise mechanism for modeling the diverse clinical symptoms of schizophrenia across the life span (Hunt *et al.*, 2017).

Importantly, chronic differences in phase-amplitude coupling were not accompanied by consistent longitudinal changes in frequency band-specific amplitudes. Compared to saline controls, chronic ketamine decreased theta and increased slow gamma, but not fast gamma amplitude. These findings are consistent with substantial evidence from acute ketamine models that demonstrate decreases in theta and increases in gamma amplitude (Lazarewicz *et al.*, 2010; Hinman *et al.*, 2012; Kittelberger *et al.*, 2012; Caixeta *et al.*, 2013).

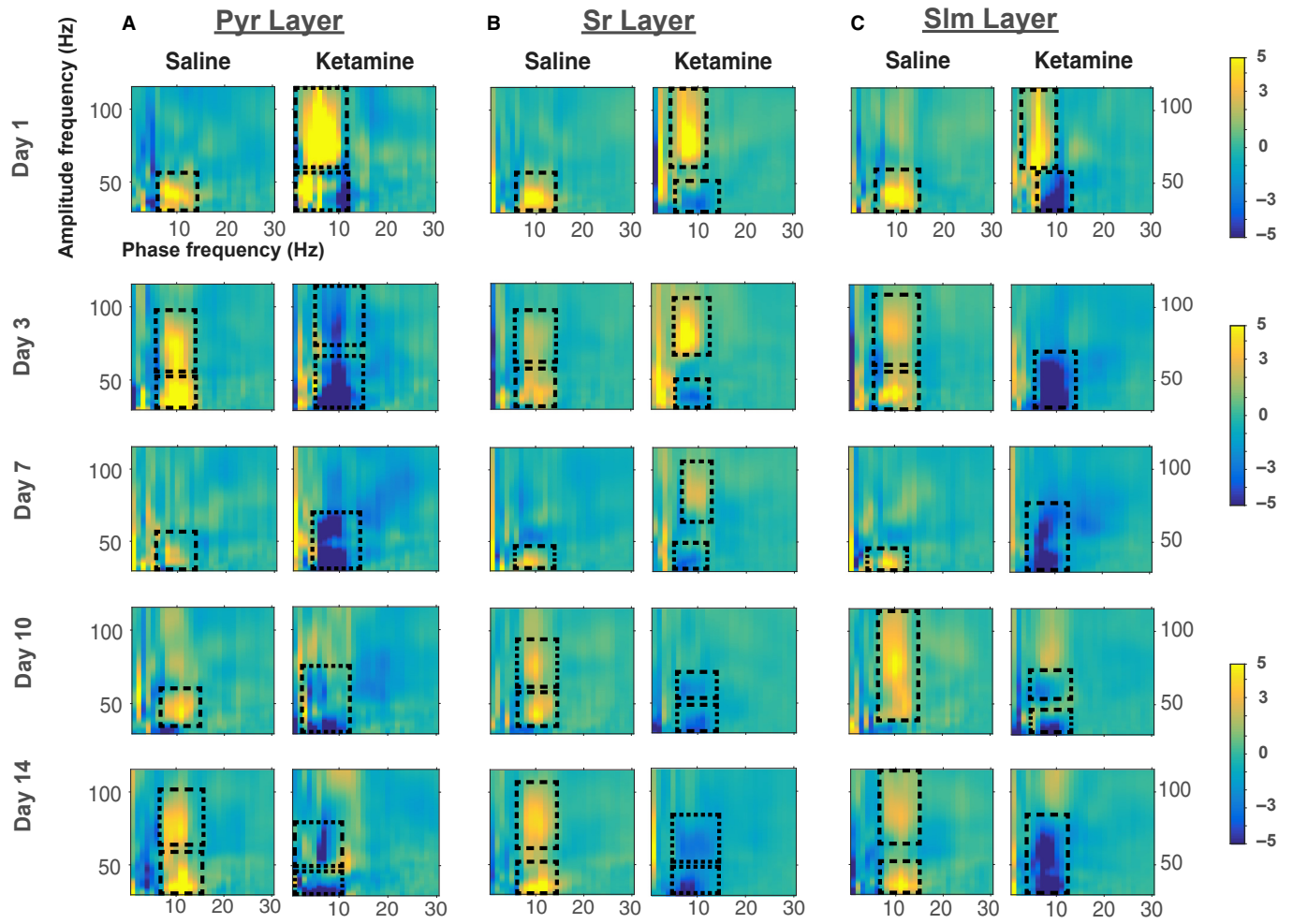

FIG. 6. Phase-amplitude cross-frequency coupling across days 1, 3, 7, 10 and 14 at slow speeds for ketamine and saline animals for all electrodes implanted across three CA1 layers (Pyr, stratum pyramidale (A); Sr, stratum radiatum (B); Slm, stratum lacunosum moleculare (C)). Each plot reflects the modulation index (MI) value after subtracting post-injection from pre-injection CFC plots. On day 1, two patterns emerge in the ketamine group, centered on slow (30–50 Hz) and fast (> 65 Hz) gamma frequencies. While there is a decrease in coupling strength from pre to post in the slow pattern, an increase occurs in the fast pattern. Across the remaining days, the coupling strength generally appears to decreases from pre to post in the ketamine group but increases in the saline group.

Yet findings from chronic models are more mixed; while Kittelberger *et al.* (2012) find chronic decreases in CA1 theta and gamma power, some (McNally *et al.*, 2013; Sullivan *et al.*, 2015; Phoumthipphavong *et al.*, 2016) report increase in gamma amplitude in cortical networks, changes in the peak frequency of gamma oscillations or no change in power. In cortical networks, chronic NMDAR antagonism does not appear to be a consequence of single-neuron activity but rather the interaction of large neuron ensembles during sensory-evoked activity (Hamm *et al.*, 2017). More subtle changes in CFC could provide a potential explanation for why some clinical studies (Symond *et al.*, 2005; Cho *et al.*, 2006) report reduced gamma power in patients with schizophrenia, while others (Tekell *et al.*, 2005; Flynn *et al.*, 2008) report increased power and some (Spencer *et al.*, 2008) report no differences. Our results also suggest that changes in amplitude are dependent upon behavioral differences; while theta amplitude decreased in the ketamine group at slow speeds, it increased at fast speeds. The largest changes were observed on days 1, 3 and 5. Although previous studies have sought to distinguish ketamine-induced changes in locomotion with oscillatory disruption, our group has previously demonstrated (Hinman *et al.*, 2012; Penley *et al.*, 2013; Long *et al.*, 2014) that novel sensory experiences can alter the relation of locomotive speed to theta and gamma characteristics. In CA3 hippocampus, acute ketamine mediates the balance between theta and gamma responses to sensory stimuli (Lazarewicz *et al.*, 2010). Differences in results may also be driven by the dosage of ketamine administered, given that the physiological, locomotive and behavioral effects of ketamine are highly dose-dependent (Imre *et al.*, 2006). Characterizing changes in coupling interactions (rather than discrete frequency bands alone) within the context of behavior may provide an explanation for inconsistent findings in both the animal and clinical literature.

There are several limitations of the present study. The study may have been underpowered to detect chronic effects given that only six animals were included with only two in control group. All of the animals in the present study were previously exposed to the behavioral task. Both theta and gamma LFP signals are increased in response to novel sensory experience (Penley *et al.*, 2013), which may have contributed to reduced ability to detect significant differences in the present study. It will be important for future studies to replicate our findings during tasks that require spatial navigation within novel environments, may lead to improved ability to identify

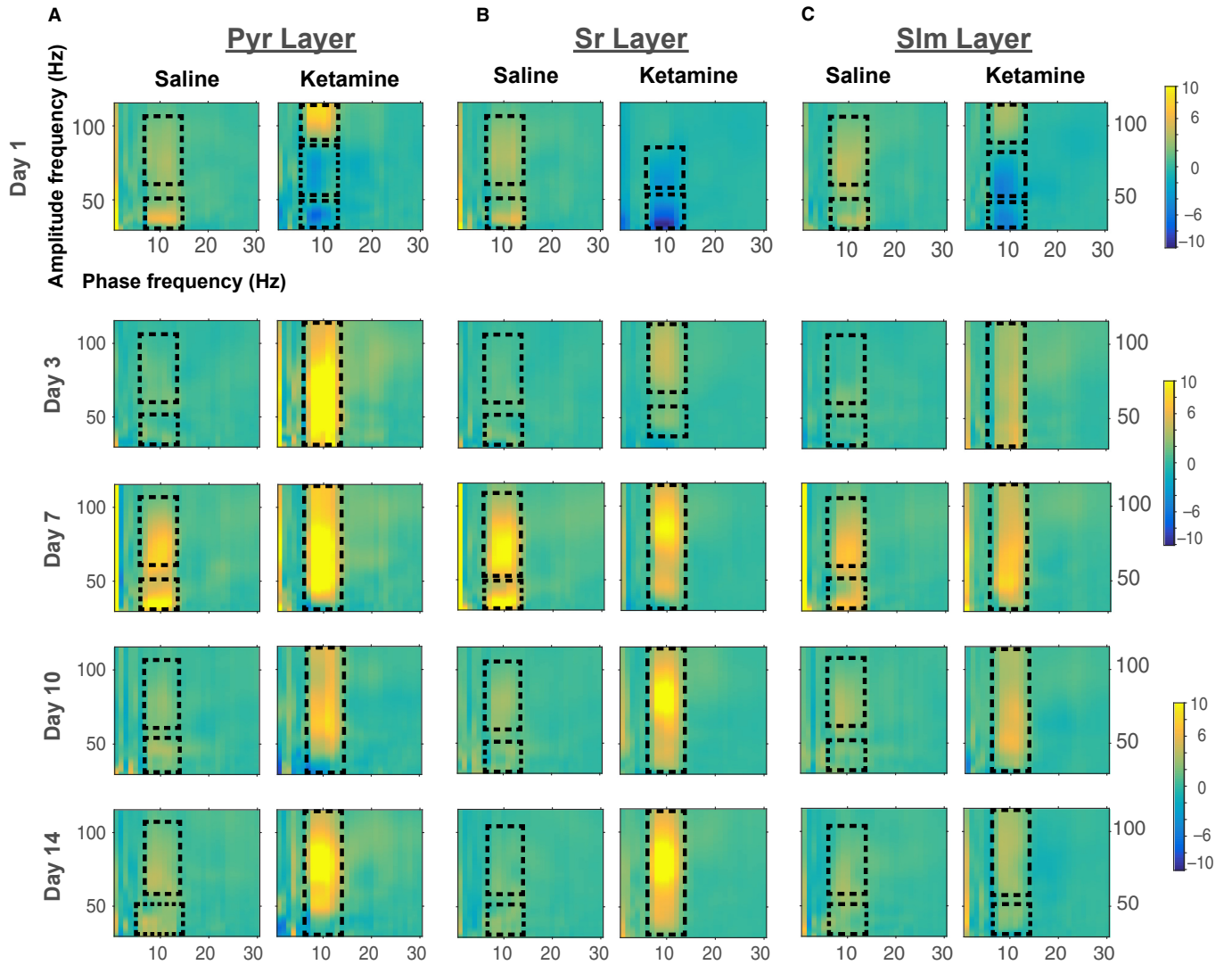

FIG. 7. Phase-amplitude cross-frequency coupling across days 1, 3, 7, 10 and 14 at fast speeds (37.5–87.0 cm/s) for ketamine and saline animals for all electrodes implanted across three CA1 layers (Pyr, stratum pyramidale; Sr, stratum radiatum; and Slm, stratum lacunosum moleculare). Each plot reflects the modulation index (MI) value after subtracting post-injection from pre-injection CFC plots. On day 1, the difference in coupling strength is negative in ketamine group but positive in the saline in all layers. On all other days, there is a larger increase in coupling strength in the ketamine group compared to the saline although the differences vary between the Pyr (A), Sr (B) and Slm (C) layers.

the functional consequences of changes in the strength and pattern of CFC upon ketamine challenge. Animals in the ketamine group had been previously exposed to the drug, potentially resulting in sensitization. However, this is unlike the case in the current study, as the previous exposure occurred several months prior to the present study, providing sufficient recovery time.

Our results suggest that chronic NMDAR antagonism alters the coupling between low-frequency phase-high-frequency amplitude in CA1 hippocampus differentially across time, by animal locomotive speed and by CA1 hippocampal layer. CFC may represent a plausible physiological mechanism for understanding the pathogenesis of information processing and memory-related cognitive deficits in schizophrenia. Hippocampal theta-gamma coupling has been suggested to represent a neural code by which multiple neural ensembles temporally represent sequential information, a process that is critical not only for information processing but for memory storage and retrieval (Lisman & Buzsáki, 2008; Canolty & Knight, 2010; Belluscio *et al.*, 2012; Kirihara *et al.*, 2012). Brain rhythms function through interaction (Canolty & Knight, 2010; Aru *et al.*, 2015), working together to generate neural coding schemes that may facilitate the timing and efficiency of neural firing required for complex perceptual and cognitive processes. In the present study, we provide additional evidence that the NMDAR hypofunction model disrupts hippocampal oscillatory coupling despite variable differences in chronic amplitude changes in specific frequency bands. NMDAR dysfunction is not only evident in the underlying pathophysiology of specific symptoms of schizophrenia, but also in disease progression. The present results provide several important directions for future research. Given the neurodevelopmental origins or schizophrenia pathology and the fact that clinical symptoms emerge during late adolescence/early adulthood, it is likely that NMDAR antagonism may exert different effects across critical periods of brain development. The present study utilized adult animals, and therefore, it will be important for future studies to examine the acute and chronic effects of ketamine of theta-gamma coupling during earlier periods of brain maturation. Future developmental approaches will be needed to improve our understanding of how neurobiological vulnerabilities alter the firing of neural populations critical for

information processing and ultimately lead to the emergence of the cognitive and perceptual abnormalities that characterize clinical symptoms (Snyder & Gao, 2013).

Acknowledgements

None.

Financial disclosure

James. J. Chrobak received financial support from National Science Foundation under the Grant number NSF 0090451. Chi-Ming Chen was honored with NARSAD Young Investigators Award of the Brain & Behavior Research Foundation.

Conflict of interest

The authors declare that the research was conducted in the absence of any commercial or financial relationships that could be construed as a potential conflict of interest.

Author contributions

C.-M.A. Chen and J.J. Chrobak designed the study. L. Long and J.J. Chrobak acquired the data. T. Michaels, L. Long, I. Stevenson and C.-M.A. Chen analyzed the data. T. Michaels and C.-M.A. Chen wrote the first draft of the manuscript. C.-M.A. Chen, I. Stevenson and J.J. Chrobak reviewed the manuscript. All authors approved its publication.

Data accessibility

The authors choose not to archive the data in the repository, as the data are part of a larger data set that is still being analyzed and may be utilized for future publications.

References

Adell, A., Jiménez-Sánchez, L., López-Gil, X. & Romón, T. (2012) Is the acute NMDA receptor hypofunction a valid model of schizophrenia? *Schizophrenia Bull.*, **38**, 9–14.

American Psychiatric Association (2013) *DSM 5*, *American Journal of Psychiatry*. American Psychiatric Publishing, Washington, DC.

Andersen, P., Morris, R., Amaral, D., Bliss, T. & O' Keefe, J. (2009). *The Hippocampus Book*. Oxford University Press, Oxford, UK.

Aru, J., Aru, J., Priesemann, V., Wibral, M., Lana, L., Pipa, G., Singer, W. & Vicente, R. (2015) Untangling cross-frequency coupling in neuroscience. *Curr. Opin. Neurobiol.*, **31**, 51–61.

Behrens, M.M., Ali, S.S., Dao, D.N., Lucero, J., Shekhtman, G., Quick, K.L. & Dugan, L.L. (2007) Ketamine-induced loss of phenotype of fast-spiking interneurons is mediated by NADPH-oxidase. *Science*, **318**, 1645–1647.

Belluscio, M.A., Mizuseki, K., Schmidt, R., Kempter, R. & Buzsáki, G. (2012) Cross-frequency phase-phase coupling between θ and γ oscillations in the hippocampus. *J. Neurosci.*, **32**, 423–435.

Bragin, A., Jando, G., Nadasdy, Z., Hetke, J., Wise, K. & Buzsaki, G. (1995) Gamma (40–100 Hz) oscillation in the hippocampus of the behaving rat. *J. Neurosci.*, **15**, 47–60.

Brébion, G., Stephan-Otto, C., Huerta-Ramos, E., Ochoa, S., Usall, J., Abellán-Vega, H., Roca, M. & Haro, J.M. (2015) Visual encoding impairment in patients with schizophrenia: contribution of reduced working memory span, decreased processing speed, and affective symptoms. *Neuropsychology*, **29**, 17.

Burgess, N. & O'Keefe, J. (2005) The theta rhythm. *Hippocampus. Spec. Issue Theta Rhythm.*

Caixeta, F.V., Cornélio, A.M., Scheffer-Teixeira, R., Ribeiro, S. & Tort, A.B.L. (2013) Ketamine alters oscillatory coupling in the hippocampus. *Sci. Rep.*, **3**, 1–10.

Canolty, R.T. & Knight, R.T. (2010) The functional role of cross-frequency coupling. *Trends Cogn. Sci.*, **14**, 506–515.

Canolty, R.T., Edwards, E., Dalal, S.S., Soltani, M., Nagarajan, S.S., Kirsch, H.E., Berger, M.S., Barbare, N.M. *et al.* (2006) High gamma power is phase-locked to theta oscillations in human neocortex. *Science*, **313**, 1626–1628.

Chang, E.H., Frattini, S.A., Robbiati, S. & Huerta, P.T. (2013) Construction of microdrive arrays for chronic neural recordings in awake behaving mice. *J. Vis. Exp.*, (77), e50470.

Cho, R.Y., Konecky, R.O. & Carter, C.S. (2006) Impairments in frontal cortical γ synchrony and cognitive control in schizophrenia. *Proc. Natl. Acad. Sci. USA*, **103**, 19878–19883.

Chrobak, J.J. & Buzsáki, G. (1998) Gamma oscillations in the entorhinal cortex of the freely behaving rat. *J. Neurosci.*, **18**, 388–398.

Colgin, L.L., Denninger, T., Fyhn, M., Hafting, T., Bonnevie, T., Jensen, O., Moser, M.-B. & Moser, E.I. (2009) Frequency of gamma oscillations routes flow of information in the hippocampus. *Nature*, **462**, 353–357.

Cunningham, M.O., Hunt, J., Middleton, S., LeBeau, F.E.N., Gillies, M.J., Davies, C.H., Maycox, P.R., Whittington, M.A. *et al.* (2006) Region-specific reduction in entorhinal gamma oscillations and parvalbumin-immunoreactive neurons in animal models of psychiatric illness. *J. Neurosci.*, **26**, 2767–2776.

Engel, A.K., Fries, P. & Singer, W. (2001) Dynamic predictions: oscillations and synchrony in top–down processing. *Nat. Rev. Neurosci.*, **2**, 704–716.

Fell, J., Klaver, P., Lehnertz, K., Grunwald, T., Schaller, C., Elger, C.E. & Fernández, G. (2001) Human memory formation is accompanied by rhinal-hippocampal coupling and decoupling. *Nat. Neurosci.*, **4**, 1259–1264.

Fleming, K., Goldberg, T.E., Binks, S., Randolph, C., Gold, J.M. & Weinberger, D.R. (1997) Visuospatial working memory in patients with schizophrenia. *Biol. Psychiat.*, **41**, 43–49.

Flynn, G., Alexander, D., Harris, A., Whitford, T., Wong, W., Galletly, C., Silverstein, S., Gordon, E. *et al.* (2008) Increased absolute magnitude of gamma synchrony in first-episode psychosis. *Schizophr. Res.*, **105**, 262–271.

Fyhn, M., Hafting, T., Treves, A., Moser, M.-B. & Moser, E.I. (2007) Hippocampal remapping and grid realignment in entorhinal cortex. *Nature*, **446**, 190–194.

Green, C., Knight, J., Precious, S. & Simpkin, S. (1981) Ketamine alone and combined with diazepam or xylazine in laboratory animals: a 10 year experience. *Lab Animal*, **15**, 163–170.

Haenschel, C., Bittner, R.A., Waltz, J., Haertling, F., Wibral, M., Singer, W., Linden, D.E.J. & Rodriguez, E. (2009) Cortical oscillatory activity is critical for working memory as revealed by deficits in early-onset schizophrenia. *J. Neurosci.*, **29**, 9481–9489.

Hafting, T., Fyhn, M., Molden, S., Moser, M.-B. & Moser, E.I. (2005) Microstructure of a spatial map in the entorhinal cortex. *Nature*, **436**, 801–806.

Hakami, T., Jones, N.C., Tolmacheva, E.A., Gaudias, J., Chaumont, J., Salzberg, M., O'Brien, T.J. & Pinault, D. (2009) NMDA receptor hypofunction leads to generalized and persistent aberrant gamma oscillations independent of hyperlocomotion and the state of consciousness. *PLoS One*, **4**, e6755.

Hamm, J.P., Peterka, D.S., Gogos, J.A. & Yuste, R. (2017) Altered cortical ensembles in mouse models of schizophrenia. *Neuron*, **94**, 153–167.

Harrison, P.J. (2004) The hippocampus in schizophrenia: a review of the neuropathological evidence and its pathophysiological implications. *Psychopharmacology*, **174**, 151–162.

Hetzler, B.E. & Swain Wautlet, B. (1985) Ketamine-induced locomotion in rats in an open-field. *Pharmacol. Biochem. Be.*, **22**, 653–655.

Hinman, J.R., Penley, S.C., Escabi, M.A. & Chrobak, J.J. (2012) Ketamine disrupts theta synchrony across the septotemporal axis of the CA1 region of hippocampus. *J. Neurophysiol.*, **109**, 570–579.

Hirai, N., Uchida, S., Maehara, T., Okubo, Y. & Shimizu, H. (1999) Enhanced gamma (30–150 Hz) frequency in the human medial temporal lobe. *Neuroscience*, **90**, 1149–1155.

Hunt, M.J., Kopell, N.J., Traub, R.D. & Whittington, M.A. (2017) Aberrant network activity in schizophrenia. *Trends Neurosci.*, **40**, 371–382.

IBM SPSS Inc (2012) SPSS Statistics for Windows. IBM Corp. Released 2012, Version 20, 1–8.

Imre, G., Fokkema, D.S., Den Boer, J.A. & Ter Horst, G.J. (2006) Dose-response characteristics of ketamine effect on locomotion, cognitive function and central neuronal activity. *Brain Res. Bull.*, **69**, 338–345.

Javitt, D.C., Zukin, S.R., Heresco-Levy, U. & Umbricht, D. (2012) Has an angel shown the way? Etiological and therapeutic implications of the PCP/NMDA model of schizophrenia. *Schizophrenia Bull.*, **38**, 958–966.

Jones, R.S.G. & Bühl, E.H. (1993) Basket-like interneurones in layer II of the entorhinal cortex exhibit a powerful NMDA-mediated synaptic excitation. *Neurosci. Lett.*, **149**, 35–39.

Jones, M.W. & Wilson, M.A. (2005) Theta rhythms coordinate hippocampal-prefrontal interactions in a spatial memory task. *PLoS Biol.*, **3**, e402.
Kirihara, K., Rissling, A.J., Swerdlow, N.R., Braff, D.L. & Light, G.A. (2012) Hierarchical organization of gamma and theta oscillatory dynamics in schizophrenia. *Biol. Psychiat.*, **71**, 873–880.
Kittelberger, K., Hur, E.E., Sazegar, S., Keshavan, V. & Kocsis, B. (2012) Comparison of the effects of acute and chronic administration of ketamine on hippocampal oscillations: relevance for the NMDA receptor hypofunction model of schizophrenia. *Brain Struct. Funct.*, **217**, 395–409.
Korotkova, T., Fuchs, E.C., Ponomarenko, A., von Engelhardt, J. & Monyer, H. (2010) NMDA receptor ablation on parvalbumin-positive interneurons impairs hippocampal synchrony, spatial representations, and working memory. *Neuron*, **68**, 557–569.
Krystal, J.H., Karper, L.P., Seibyl, J.P., Freeman, G.K., Delaney, R., Bremner, J.D., Heninger, G.R. & Bowers, M.B. *et al.* (1994) Subanesthetic Effects of the Noncompetitive NMDA Antagonist, Ketamine, in Humans Psychotomimetic, Perceptual, Cognitive, and Neuroendocrine Responses. *Arch. Gen. Psychiat.*, **51**, 199–214.
Lakhan, S.E. & Vieira, K.F. (2009) Schizophrenia pathophysiology: are we any closer to a complete model? *Ann. Gen. Psychiatr.*, **8**, 12.
Lazarewicz, M.T., Ehrlichman, R.S., Maxwell, C.R., Gandal, M.J., Finkel, L.H. & Siegel, S.J. (2010) Ketamine modulates theta and gamma oscillations. *J. Cognitive Neurosci.*, **22**, 1452–1464.
Leicht, G., Vauth, S., Polomac, N., Andreou, C., Rauh, J., Mußmann, M., Karow, A. & Mulert, C. (2016) EEG-informed fMRI reveals a disturbed gamma-band-specific network in subjects at high risk for psychosis. *Schizophrenia Bull.*, **42**, 239–249.
Leung, L.S. & Shen, B. (2004) Glutamatergic synaptic transmission participates in generating the hippocampal EEG. *Hippocampus*, **14**, 510–525.
Lisman, J. & Buzsáki, G. (2008) A neural coding scheme formed by the combined function of gamma and theta oscillations. *Schizophrenia Bull.*, **34**, 974–980.
Long, L.L., Hinman, J.R., Stevenson, I.H., Read, H.L., Escabi, M.A. & Chrobak, J.J. (2014) Novel acoustic stimuli can alter locomotor speed to hippocampal theta relationship. *Hippocampus*, **24**, 1053–1058.
Long, L.L., Bunce, J.G. & Chrobak, J.J. (2015) Theta variation and spatiotemporal scaling along the septotemporal axis of the hippocampus. *Front. Syst. Neurosci.*, **9**, 1–14.
Long, L.L., Podurgiel, S.J., Haque, A.F., Errante, E.L., Chrobak, J.J. & Salamone, J.D. (2016) Subthalamic and cortical local field potentials associated with pilocarpine-induced oral tremor in the rat. *Front. Behav. Neurosci.*, **10**, 1–12.
Ma, J. & Leung, L.S. (2007) The supramammillo-septal-hippocampal pathway mediates sensorimotor gating impairment and hyperlocomotion induced by MK-801 and ketamine in rats. *Psychopharmacology*, **191**, 961–974.
MathWorks (2014) MATLAB and Signal Processing Toolbox, Version R2014a [WWW Document]. Massachusetts, USA. Available http://www.mathworks.com/products/connections/?refresh=true.
McDougall, S.A., Moran, A.E., Baum, T.J., Apodaca, M.G. & Real, V. (2017) Effects of ketamine on the unconditioned and conditioned locomotor activity of preadolescent and adolescent rats: impact of age, sex, and drug dose. *Psychopharmacology*, **234**, 2683–2696.
McNally, J.M., McCarley, R.W. & Brown, R.E. (2013) Chronic ketamine reduces the peak frequency of gamma oscillations in mouse prefrontal cortex ex vivo. *Front. Psychiat.*, **4**, 106.
Miller, E.K. & Cohen, J.D. (2001) An integrative theory of prefrontal cortex function. *Annu. Rev. Neurosci.*, **24**, 167–202.
Penley, S.C., Hinman, J.R., Long, L.L., Markus, E.J., Escabí, M.A. & Chrobak, J.J. (2013) Novel space alters theta and gamma synchrony across the longitudinal axis of the hippocampus. *Front. Syst. Neurosci.*, **7**, 20.
Phoumthipphavong, V., Barthas, F., Hassett, S. & Kwan, A.C. (2016) Longitudinal effects of ketamine on dendritic architecture in vivo in the mouse medial frontal cortex. *eNeuro*, **3**, ENEURO.0133-15.2016.
R Core Team (2013) R Development Core Team. *R A Lang. Environ. Stat. Comput.*, **55**, 275–286.
Roopun, A.K., Cunningham, M.O., Racca, C., Alter, K., Traub, R.D. & Whittington, M.A. (2008) Region-specific changes in gamma and beta2 rhythms in NMDA receptor dysfunction models of schizophrenia. *Schizophrenia Bull.*, **34**, 962–973.
Scheffer-Teixeira, R., Belchior, H., Caixeta, F.V., Souza, B.C., Ribeiro, S. & Tort, A.B.L. (2012) Theta phase modulates multiple layer-specific oscillations in the CA1 region. *Cereb. Cortex*, **22**, 2404–2414.
Schmiedt, C., Brand, A., Hildebrandt, H. & Basar-Eroglu, C. (2005) Event-related theta oscillations during working memory tasks in patients with schizophrenia and healthy controls. *Cognitive Brain Res.*, **25**, 936–947.
Silver, H. & Goodman, C. (2008) Verbal as well as spatial working memory predicts visuospatial processing in male schizophrenia patients. *Schizophr. Res.*, **101**, 210–217.
Sirota, A., Montgomery, S., Fujisawa, S., Isomura, Y., Zugaro, M. & Buzsáki, G. (2008) Entrainment of neocortical neurons and gamma oscillations by the hippocampal theta rhythm. *Neuron*, **60**, 683–697.
Snyder, M.A. & Gao, W.J. (2013) NMDA hypofunction as a convergence point for progression and symptoms of schizophrenia. *Front. Cell Neurosci.*, **7**, 31.
Spencer, K.M., Salisbury, D.F., Shenton, M.E. & McCarley, R.W. (2008) Gamma-band auditory steady-state responses are impaired in first episode psychosis. *Biol. Psychiat.*, **64**, 369–375.
Steffenach, H.-A., Sloviter, R.S., Moser, E.I. & Moser, M.-B. (2002) Impaired retention of spatial memory after transection of longitudinally oriented axons of hippocampal CA3 pyramidal cells. *Proc. Natl. Acad. Sci. USA*, **99**, 3194–3198.
Sullivan, E.M., Timi, P., Hong, L.E. & O'Donnell, P. (2015) Reverse translation of clinical electrophysiological biomarkers in behaving rodents under acute and chronic NMDA receptor antagonism. *Neuropsychopharmacol.*, **40**, 719–727.
Sutherland, R.J., Whishaw, I.Q. & Kolb, B. (1983) A behavioural analysis of spatial localization following electrolytic, kainate- or colchicine-induced damage to the hippocampal formation in the rat. *Behav. Brain Res.*, **7**, 133–153.
Swanson, L.W. & Cowan, W.M. (1977) An autoradiographic study of the organization of the efferent connections of the hippocampal formation in the rat. *J. Comp. Neurol.*, **172**, 49–84.
Symond, M.B., Harris, A.W.F., Gordon, E. & Williams, L.M. (2005) "Gamma synchrony" in first-episode schizophrenia: a disorder of temporal connectivity? *Am. J. Psychiat.*, **162**, 459–465.
Tekell, J.L., Hoffmann, R., Hendrickse, W., Greene, R.W., Rush, A.J. & Armitage, R. (2005) High frequency EEG activity during sleep: characteristics in schizophrenia and depression. *Clin. EEG Neurosci.*, **36**, 25–35.
Tort, A.B.L., Komorowski, R., Eichenbaum, H. & Kopell, N. (2010) Measuring phase-amplitude coupling between neuronal oscillations of different frequencies. *J. Neurophysiol.*, **104**, 1195–1210.
Tsien, J.Z., Huerta, P.T. & Tonegawa, S. (1996) The essential role of hippocampal CA1 NMDA receptor-dependent synaptic plasticity in spatial memory. *Cell*, **87**, 1327–1338.
Uhlhaas, P.J. & Singer, W. (2010) Abnormal neural oscillations and synchrony in schizophrenia. *Nat. Rev. Neurosci.*, **11**, 100–113.
Vertes, R.P. (2005) Hippocampal theta rhythm: a tag for short-term memory. *Hippocampus*, **15**, 923–935.
Ward, L.M. (2003) Synchronous neural oscillations and cognitive processes. *Trends Cogn. Sci.*, **7**, 553–559.
Williams, L.M., Whitford, T.J., Nagy, M., Flynn, G., Harris, A.W.F., Silverstein, S.M. & Gordon, E. (2009) Emotion-elicited gamma synchrony in patients with first-episode schizophrenia: a neural correlate of social cognition outcomes. *J. Psychiatr. Neurosci.*, **34**, 303–313.
Wilson, T.W., Hernandez, O.O., Asherin, R.M., Teale, P.D., Reite, M.L. & Rojas, D.C. (2008) Cortical gamma generators suggest abnormal auditory circuitry in early-onset psychosis. *Cereb. Cortex*, **18**, 371–378.
Wong, A.H.C. & Josselyn, S.A. (2016) Caution when diagnosing your mouse with schizophrenia: the use and misuse of model animals for understanding psychiatric disorders. *Biol. Psychiat.*, **79**, 32–38.